THE BELL SYSTEM TECHNICAL JOURNAL
Vol. 57, No. 8, October 1978
Printed in U.S.A.

Free Electron Laser

by A. HASEGAWA

(Manuscript received March 6, 1978)

An introductory guide to the basic mechanisms of the free electron laser is presented. The laser gain originates from the stimulated Raman or Compton backscattering of a pump electromagnetic field by a relativistic electron beam. The condition of optimization of the gain, the maximum operation frequency, and the optimum output power are obtained in terms of the beam parameters and the magnitude of the pump magnetic field.

I. INTRODUCTION

Recent observations of amplification of submillimeter[1] and infrared[2] electromagnetic waves using a relativistic electron beam (REB) have created interest in applying the mechanism to produce a high-power, tunable laser in the infrared to visible range as well as in speculating the possibility of constructing an X-ray laser.

This paper introduces the basic mechanism of the amplification processes and discusses the limitations in the power and frequency referring to the presently available REBs. A nonspecialist should be able to follow the contents without referring to special references.

Section II introduces Lorentz transformation of various variables between the beam and the laboratory frames, which are used in succeeding sections.

One of the important discussions presented here is the distinction between the stimulated Compton and stimulated Raman scattering. When the scattering occurs by an excitation of a single particle state, uncorrelated free-streaming motion of electrons, it is called the stimulated Compton scattering; if it occurs by an excitation of plasmon, the collective plasma oscillation of the electrons, it is called the stimulated Raman scattering. In most cases, the stimulated Compton scattering has a gain which is too small to be useful for practical purposes. Hence, the limitation in the output frequency is decided by whether or not the relativistic electron beam can be operated in the stimulated Raman regime. The beam current density and the energy spread is the decisive factor for this, as shown in Section III.

The gain calculations based on classic mechanics are presented for both processes in Sections IV and V. The classic calculation is justified when the scattered photon density is large so that the photons can be regarded as consisting of a continuous fluid. This occurs when the number of photons in a box of its wavelength (λ) cubed is much larger than unity; that is, when $\lambda^3 P/(\hbar\omega c) \gg 1$, where P is the electromagnetic power and c is the speed of light.

Some design examples using presently available REBs are shown in Section IV. MKS units are used throughout this paper. Definitions of the notations and subscripts used are listed below.

z: coordinate taken in the direction of the beam velocity.
x, y: coordinates perpendicular to the beam velocity
m: electron rest mass
p: momentum
P: power
$\mathbf{v}_0$: beam velocity
$\mathbf{v}_g$: group velocity
E: electric field intensity
B: magnetic flux density
c: speed of light, 3×10^8 m/s
γ: $(1 - v_0^2/c^2)^{-1/2}$ [eq. (5)]
H_0: beam energy
γ_0: H_0/mc^2 [eq. (21)]
ω_p: plasma angular frequency, frame invariant
k_0: $2\pi/\lambda_0$ (λ_0 is the periodicity of the helical winding of the pump magnetic field, Fig. 1)
ω_0: $k_0 c$
ϵ_0: space dielectric constant, 8.854×10^{-12} F/m
v_T: thermal speed in the beam frame [eq (17) and (35)]
$\Delta\gamma/\gamma$: relative energy spread of the beam in the laboratory frame
Γ: temporal gain
ω_i: incident electromagnetic wave angular frequency, which corresponds to the pump frequency in the beam frame
k_i: incident wavenumber, beam frame
ω_s: scattered electromagnetic wave angular frequency, beam frame
k_s: scattered wavenumber, beam frame
ω_l: longitudinal electrostatic wave angular frequency, beam frame
k_l: longitudinal wavenumber, beam frame
$B_\perp$: transverse pump magnetic field, laboratory frame
k_D: Debye wavenumber ω_p/v_T in the beam frame
ω_{cr}: angular frequency of transition from stimulated Raman to

stimulated Compton scattering in the laboratory frame [eq. (37)]

J_0: beam current density

v_i: amplitude of oscillating velocity of electrons due to the incident (pump) wave [eq. (24)]

Subscript L: quantities in the laboratory frame
Subscript B: quantities in the beam frame
Subscript l: longitudinal wave, beam frame
Subscript s: scattered wave, beam frame
Subscript i: incident wave, beam frame
Subscript $\perp$: component perpendicular to z.

II. LORENTZ TRANSFORMATIONS

To understand the dynamics of the REB, we must first refresh our memory of the Lorentz transformations which are relevant to our problem. If we take z axis in the direction of the beam velocity as in Fig. 1 and use subscripts L and B to represent the laboratory and the beam frame, the Lorentz transformations of the coordinate z and time t for a REB with the velocity v_0 are given by (for example, see Ref. 3):

$$z_B = \gamma(z_L - v_0 t_L) \tag{1}$$

or

$$z_L = \gamma(z_B + v_0 t_B), \tag{2}$$

and

$$t_B = \gamma \left(t_L - \frac{v_0}{c^2} z_L \right), \tag{3}$$

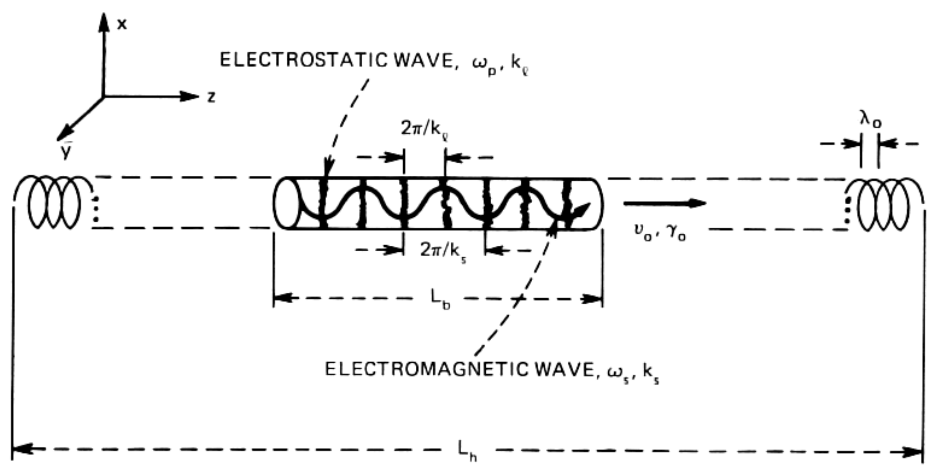

Fig. 1—Schematic diagram of a free electron laser which utilizes the helical magnetic pump field. The helical current produces a periodic magnetic field which induces longitudinal electrostatic oscillations in the beam. A nonlinear interaction between the induced longitudinal oscillation and the periodic pump field produces an electromagnetic wave which propagates in the direction of the beam. This process can be viewed, in the beam frame, as a stimulated backscattering of the pump field by the electrons in the beam. Since the scattered wave propagates at the same speed as the beam itself, the beam length, L_b, can be a size of several wavelengths in the beam frame. However, the length of the helical field, L_h, should be such that enough e-folding gain can be obtained. The minimum e-folding distance is obtained in eq. (91). L_h should therefore be much larger than L_m in this equation. Typically, L_m is on the order of 1 m.

or

$$t_L = \gamma\left(t_B + \frac{v_0}{c^2} z_B\right), \tag{4}$$

where

$$\gamma = \left(1 - \frac{v_0^2}{c_2}\right)^{-1/2} \tag{5}$$

and c is the speed of light. Similarly, the electric field intensity **E** and the magnetic flux density **B** are transformed to

$$E_{Bz} = E_{Lz}, \tag{6}$$

$$\mathbf{E}_{B\perp} = \gamma(\mathbf{E}_{L\perp} + \mathbf{v}_0 \times \mathbf{B}_L), \tag{7}$$

and

$$B_{Bz} = B_{Lz}, \tag{8}$$

$$\mathbf{B}_{B\perp} = \gamma\left(\mathbf{B}_{L\perp} - \frac{1}{c^2}\mathbf{v}_0 \times \mathbf{E}_L\right), \tag{9}$$

where subscript $\perp$ shows the component perpendicular to the beam velocity. Equation (7) indicates that a transverse magnetic field which is static but spacially periodic in the z direction with the periodicity $2\pi/k_0$ creates an oscillating electric field in the beam frame with the frequency given by $\gamma k_0 v_0$. Transformations of velocities are obtained by taking the derivatives of (2) and (4),

$$v_{Lz} = \frac{v_{Bz} + v_0}{1 + v_0 v_{Bz}/c^2}. \tag{10}$$

The beam has transverse velocity modulation due to the $\mathbf{v}_0 \times \mathbf{B}_{L\perp}$ Lorentz force. The Lorentz transformation becomes

$$v_{L\perp} = \frac{v_{B\perp}}{\gamma(1 + v_0 v_{Bz}/c^2)} \simeq \frac{1}{\gamma} v_{B\perp}. \tag{11}$$

The Lorentz transformations for frequency and the wave number are obtained by considering the phase factor $k_L z_L + \omega_L t_L$ of a wave in the laboratory frame, exp i$(kz + \omega t)$; we take a wave propagating against the beam direction to consider the back scattering.

$$k_L z_L + \omega_L t_L = \gamma\left(k_L + \frac{v_0}{c^2}\omega_L\right) z_B + \gamma(\omega_L + k_L v_0) t_B; \tag{12}$$

hence

$$k_B = \gamma\left(k_L + \frac{v_0}{c^2}\omega_L\right), \tag{13}$$

$$\omega_B = \gamma(\omega_L + k_L v_0). \tag{14}$$

One important aspect of this result is that the frequency seen by the beam is γ times the laboratory frequency ω_L *plus* γ times the Doppler shifted laboratory frequency $k_L v_0$. An electromagnetic pump wave propagating against the beam direction (whose dispersion relation is given by $\omega = kc$) has a frequency given by $\gamma(\omega + kv_0) \simeq 2\gamma\omega$ when observed in the beam frame. Similarly, the frequency ω_s of the back-scattered light which faces little frequency shift from the incident light in the beam frame becomes $2\gamma\omega_s$ when observed in the laboratory frame. Hence, the frequency of the back-scattered light in the laboratory frame is given approximately by $4\gamma^2$ times the incident (pump) frequency in the laboratory frame.

The pump frequency can be dc when a periodic magnetic field is used. In this case, the frequency of the scattered wave is given by $2\gamma^2 k_0 v_o$, where k_0 is the wave number of the periodicity λ_0, $k_0 = 2\pi/\lambda_0$, of the magnetic field (see Fig. 1).

In addition to these quantities, we need the transformation of the plasma frequency, ω_p, the beam thermal speed v_T, the beam oscillating velocity in the transverse direction due to the pump field $v_\perp$, and the growth rate Γ.

Since the Lorentz contraction increases the density by γ and the mass also by a factor γ, the plasma frequency, ω_p $(= e^2 n/\epsilon_0 m)^{1/2}$ (where e is the electron change, n the beam density, and ϵ_0 the space dielectric constant), is frame invariant.

The thermal speed in the beam frame v_T can be expressed in terms of the energy spread of the beam in the laboratory frame as follows. From the definition of γ in (5),

$$v_0^2 = c^2\left(1 - \frac{1}{\gamma^2}\right). \tag{5$'$}$$

Hence the velocity spread δv_0 in the laboratory frame is expressed in terms of the spread in γ,

$$\delta v_0 = c\,\frac{\Delta\gamma}{\gamma^3}. \tag{15}$$

Now if we use the Lorentz transformation of v_z, (10),

$$\begin{aligned}\delta v_0 = \delta v_{Lz} &= \frac{\Delta v_{Bz}}{\gamma^2(1 + v_0 v_{Bz}/c^2)}\\ &\simeq \frac{1}{\gamma^2}\,\Delta v_{Bz} = \frac{v_T}{\gamma^2},\end{aligned} \tag{16}$$

because $v_{Bz} = 0$. Hence from (16) the thermal speed in the beam frame is obtained:

$$v_T = c\,\frac{\Delta\gamma}{\gamma}. \tag{17}$$

Next, we obtain the oscillating transverse velocity in the beam frame. We consider the example of periodic magnetic pump. In this case, the beam kinetic energy H_0 does not change due to the presence of the pump. If we introduce γ_0 to represent the total kinetic energy of the beam,

$$\begin{aligned} H_0 &= c(p_L^2 + m^2c^2)^{1/2} \\ &\equiv mc^2\gamma_0, \end{aligned} \tag{18}$$

where p_L is the momentum in the laboratory frame (H_0 is not frame invariant, but we delete subscript L for this quantity). The velocity components in the transverse and z directions are obtained in terms of p_L as

$$v_{L\perp} = \frac{\partial H_0}{\partial p_{L\perp}} = \frac{1}{m\gamma_0} p_{L\perp} \tag{19}$$

$$v_{Lz} = v_0 = \frac{1}{m\gamma_0} P_{Lz}. \tag{20}$$

If we substitute (19) and (20) into (17), we can obtain the relation between γ_0 and γ as defined in (5),

$$\gamma_0^2 = \gamma^2 \left(1 + \gamma_0^2 \frac{v_{L\perp}^2}{c^2}\right). \tag{21}$$

This expression shows that γ can be significantly different from γ_0 even if $v_{L\perp}^2/c^2 \ll 1$. With these preparations, we can now obtain $v_{B\perp}$ in terms of the pump magnetic field. The equation of motion of an electron in the presence of a transverse helical pump magnetic field $\mathbf{B}_\perp$ ($B_\perp \cos k_0z$, $B_\perp \sin k_0z$, 0) is given by

$$\frac{d\mathbf{p}_{L\perp}}{dt} = m\gamma_0 \frac{d\mathbf{v}_{L\perp}}{dt} = -e(\mathbf{v}_0 \times \mathbf{B}_\perp), \tag{22}$$

since γ_0 is constant. If we assume $v_0 \gg v_{L\perp}$, $z = v_0t$, (22) can be immediately integrated to give

$$v_{L\perp} = \left(\frac{eB_\perp}{m\gamma_0k_0} \cos (k_0v_0t), \frac{eB_\perp}{m\gamma_0k_0} \sin (k_0v_0t), 0\right). \tag{23}$$

As will be seen, we need only the magnitude of the oscillating velocity in the beam frame, $|v_{B\perp}|$, which may be obtained from (23) and (11),

$$|v_{B\perp}| = \frac{\gamma eB_\perp}{\gamma_0 mk_0} (= v_i). \tag{24}$$

This gives the relation between the oscillation amplitude of the electrons in the beam frame and the pump magnetic field in the laboratory frame.

We now consider the transformation of the growth rate Γ. If a wave with slowly varying amplitude $A_B(z_B,t_B)$ grows in time and space at a temporal growth rate Γ_B in the beam frame, A_B satisfies the following equation

$$\frac{\partial A_B}{\partial t} + v_{Bg}\frac{\partial A_B}{\partial z_B} = \Gamma_B A_B, \tag{25}$$

where v_{Bg} is the group velocity in the beam frame. If we use (2) and (4), $\partial/\partial t_B$ and $\partial/\partial z_B$ can be expressed in terms of derivatives in the laboratory frame.

$$\frac{\partial}{\partial t_B} + v_{Bg}\frac{\partial}{\partial z_B} = \gamma\left(1 + \frac{v_{Bg}v_0}{c^2}\right)\frac{\partial}{\partial t_L} + \gamma(v_0 + v_{Bg})\frac{\partial}{\partial z_L}. \tag{26}$$

If we substitute (26) into (25), we see

$$\frac{\partial A_B}{\partial t_L} + \frac{v_0 + v_{Bg}}{1 + v_{Bg}v_0/c^2}\frac{\partial A_B}{\partial z_L} = \frac{\Gamma_B}{\gamma(1 + v_{Bg}v_0/c^2)}A_B. \tag{27}$$

The amplitude in the laboratory frame is linearly proportional to A_B. Hence (27) gives the Lorentz transformation of the group velocity as well as the growth rate, i.e.,

$$v_{Lg} = \frac{v_0 + v_{Bg}}{1 + v_{Bg}v_0/c^2} \simeq \frac{1}{2}(v_0 + v_{Bg}), \tag{28}$$

$$\Gamma_L = \frac{\Gamma_B}{\gamma(1 + v_{Bg}v_0/c^2)} \simeq \frac{\Gamma_B}{2\gamma}. \tag{29}$$

III. STIMULATED COMPTON OR STIMULATED RAMAN SCATTERING?

We consider here the basic processes of the stimulated scattering *in the beam frame.* If we designate the frequency and wave number of the incident (pump) wave by ω_i and k_i and those of the scattered (amplified) wave by ω_s and k_s, the frequency and wave number of the longitudinal oscillation excited in the beam (which is a stationary electron plasma in the beam frame) are given by

$$\omega_l = \omega_i - \omega_s, \tag{30}$$

$$\mathbf{k}_l = \mathbf{k}_i - \mathbf{k}_s. \tag{31}$$

We note here that the incident and scattered waves are electromagnetic waves, hence $\omega_i/k_i \approx \omega_s/k_s \approx c$, while the longitudinal wave in the electron plasma has a phase velocity, ω_l/k_l, much smaller than the speed of light.

To consider the backscattering, which is needed to utilize the frequency up conversion as discussed in Section II, as well as to maximize the gain, we must take $\mathbf{k}_s \cdot \mathbf{k}_i = -|k_s||k_i|$. The incident wave propagates against the beam direction, hence $\mathbf{k}_i = -|k_i|\hat{\mathbf{z}}$. Thus $|k_l| = |k_s| + |k_i|$.

Now the longitudinal mode in the electron beam has the plasma dispersion relation given by

$$1 - \frac{\omega_p^2}{k_l^2} \int_{-\infty}^{\infty} \frac{\partial f_0/\partial v}{v - (\omega + i0)/k_l} dv = 0, \tag{32}$$

where $f_0(v)$ is the velocity distribution function of the beam electrons in the beam frame and is assumed to be nonrelativistic. If we solve (32) for ω, we have

$$\omega \simeq \omega_p \qquad \text{if } k_l \ll k_D, \tag{33}$$

$$\omega \simeq k_l v_T [1 - i0(1)] \qquad \text{if } k_l \gg k_D, \tag{34}$$

where

$$v_T = \left[\int_{-\infty}^{\infty} v^2 f_0 dv \right]^{1/2} \tag{35}$$

is the thermal speed of the electrons and $k_D = \omega_p/v_T$ is the Debye wave number, both in the beam frame. Equations (33) and (34) indicate that if the wave number is larger than the Debye wave number, the collective property of the plasms oscillation is lost. The large imaginary part in (34) is the consequence of the Landau damping.

Now the dispersion relation of the electromagnetic wave is given by

$$\omega^2 = c^2 k^2 + \omega_p^2. \tag{36}$$

If we use the dispersion relations for ω_i and ω_s [which satisfies (36)] and ω_l [which satisfies (32)], the resonant conditions, Eqs. (31) and (32), can be plotted in (ω,k) diagram. For the case of backscattering, the plots are shown in Fig. 2 (for the case of $k_l \ll k_D$) and Fig. 3 (for the case of $k_l \gg k_D$). In these figures, the arrows show the direction in which the state with energy $\hbar\omega_i$ and momentum $\hbar k_i$ decays into two other states with energy $\hbar\omega_s$, and $\hbar\omega_l$ and momentum $\hbar k_s$ and $\hbar k_l$. The decay process shown in Fig. 2 describes the stimulated Raman scattering and that in Fig. 3 the stimulated Compton scattering.

Both figures show backscattering because k_i and k_s have opposite signs. We see from these figures that if $\omega_s \gg \omega_p$, $|k_l| \simeq 2|k_s|$. Hence for a given quality of a beam if $\omega_s (= k_s c)$ is increased, k_l which may be initially smaller than k_D becomes larger than k_D at some value of ω_s. Hence, there exists a critical frequency of the scattered wave (which corresponds to the lasing frequency in the beam frame) above (below) which scattering process becomes Compton (Raman). If we write this critical angular frequency in the laboratory frame as ω_{cr}, that is, the actual lasing frequency, ω_{cr} can be expressed in terms of the beam quality. Using

$$\omega_{cr} = 2\gamma\omega_s$$
$$\omega_s = ck_s$$
$$k_l = 2k_s = k_D,$$

we have, with eq. (17),

$$\begin{aligned} \omega_{cr} &= \gamma k_D c \\ &= \gamma\omega_p(\gamma/\Delta\gamma). \end{aligned} \tag{37}$$

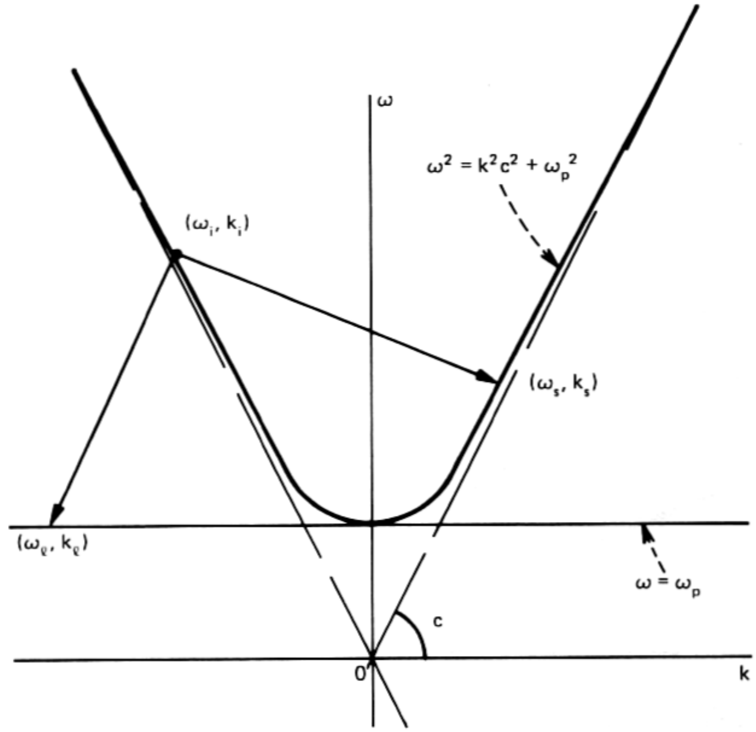

Fig. 2—Dispersion diagram of the electromagnetic wave and plasma wave in the beam frame. This diagram shows the stimulated Raman scattering process. The arrow indicates the direction of decay of the incident wave with frequency and wave number given by ω_i, k_i into a longitudinal oscillation with frequency ω_p and wavenumber k_l and a backscattered electromagnetic wave with frequency ω_s and wavenumber k_s.

Thus the critical frequency depends on the relative spread of the beam energy observed in the laboratory frame, $\Delta\gamma/\gamma$, as well as the beam density and γ. Since the plasma frequency is frame-invariant, it may be expressed in terms of the current density J_0 of the beam. Equation (37) then becomes

$$\omega_{cr} = 8.14 \times 10^6 \, \gamma(\gamma/\Delta\gamma)J_0{}^{1/2}. \tag{37'}$$

Since MKS units are used, J_0 is in the unit of A/m^2. This expression is an important criterion in designing the laser, because at $\omega > \omega_{cr}$ it should operate in the stimulated Compton regime and the growth rate becomes pessimistically small. For a practical purpose, $\omega = \omega_{cr}$ is the high-frequency limitation of a free electron laser.

IV. THE STIMULATED RAMAN SCATTERING

In this section, we derive the growth rate in the stimulated Raman regime. A number of authors have derived the growth rate using different methods. The classic mechanical calculation is much simpler than the quantum mechanical one and is well justified for a stimulated process because a large number of photons are produced at a very early stage of the process. Tytovich's book[4] and a review paper by Kaw et al.[4] are some of the appropriate references on this subject.

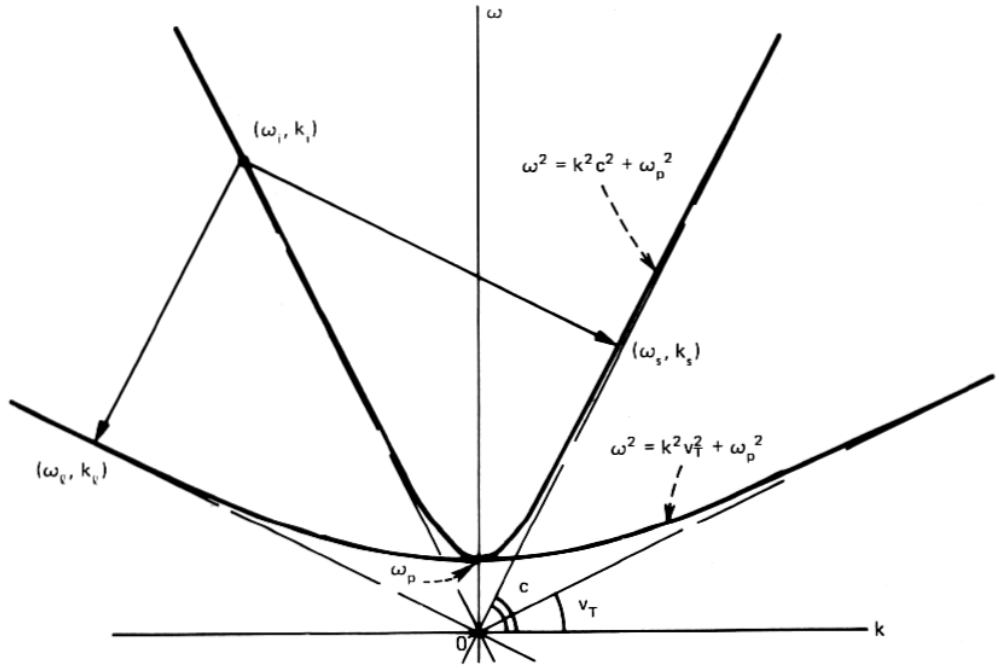

Fig. 3—The dispersion diagram that shows the stimulated Compton scattering process. When the wave number of the induced longitudinal oscillation k_l is larger than the Debye wave number k_D, the induced longitudinal oscillation in the beam electrons becomes uncorrelated. In this case, the scattering occurs by the sum of Compton scattering by individual electrons. Since the induced wave number k_l is proportional to the lasing frequency, when the lasing frequency is increased, the scattering process changes from the stimulated Raman to the stimulated Compton.

Attempts have been made to obtain the gain in the laboratory frame using a rather complicated nonlinear relativistic dynamics.[6,7] As has been shown, the gain and all the other parameters can be Lorentz-transformed into the laboratory frame, it is much simpler to do the nonrelativistic calculation in the beam frame. Thus we do the analysis in the beam frame. Referring to Fig. 2, we consider a large amplitude incident wave propagating in the negative z-direction with transverse electric field given by

$$\mathrm{Re} E_i \exp i(k_i z + \omega_i t), \tag{38}$$

where k_i and ω_i are positive. E_i is related to the pump field in the laboratory frame through the Lorentz transformation shown in eq. (7). In particular, if the static periodic magnetic field is used, E_i is given by

$$|E_i| = \gamma v_0 B_L \simeq \gamma c B_L, \tag{39}$$

where B_L is the amplitude of the rippled or helical magnetic field in the direction perpendicular to the beam.

To simplify the analysis, we assume the variation of E_i and all the other field quantities in the transverse direction is negligible. This assumption may be justified if the beam diameter is much larger than all the wavelengths involved.

To obtain the growth rate, we consider a test electromagnetic wave (the scattered wave) which propagates in the direction of the beam and which is excited by a nonlinear current density produced by the product of the incident field and the induced longitudinal density perturbation in the beam.

From the Maxwell equation, the electric field of the scattered wave $\mathbf{E}_s$ satisfies the wave equation

$$\nabla^2 \mathbf{E}_s - \frac{1}{c^2}\frac{\partial^2 \mathbf{E}_s}{\partial t^2} = \mu_0 \frac{\partial \mathbf{J}_s}{\partial t}, \tag{40}$$

where the current density consists of the linear (self-consistent) portion, $\mathbf{J}_s^L$, and the nonlinear portion $\mathbf{J}_s^{NL}$, which is produced by the incident field,

$$\mathbf{J}_s = \mathbf{J}_s^L + \mathbf{J}_s^{NL}, \tag{41}$$

where

$$\mathbf{J}_s^L = -en_0\mathbf{v}_s \tag{42}$$

and

$$\mathbf{J}_s^{NL} = -en_l\mathbf{v}_i. \tag{43}$$

$\mathbf{v}_s$ is the electron velocity modulation due to the scattered field

$$\frac{d\mathbf{v}_s}{dt} = -\frac{e}{m}\mathbf{E}_s, \tag{44}$$

while $\mathbf{v}_i$ is the modulation due to the pump field. In the case of a helical field pump, $\mathbf{v}_i$ is given by eq. (24),

$$\mathbf{v}_i = \frac{\gamma e \mathbf{B}_\perp}{\gamma_0 m k_0}, \tag{45}$$

and n_l is the density modulation due to the induced longitudinal oscillation in the beam, which satisfies the continuity equation,

$$\frac{\partial n_l}{\partial t} + \nabla \cdot (n_0 \mathbf{v}_l) = 0, \tag{46}$$

with

$$\frac{d\mathbf{v}_l}{dt} = -\frac{e}{m}\mathbf{E}_l. \tag{47}$$

$\mathbf{E}_l$ is the electric field of the longitudinal oscillation.

If we Fourier-transform (43), $\mathbf{J}_s^{NL}$ contains two frequency components, one the Stokes mode, $\omega_i - \omega$ and the other the anti-Stokes mode, $\omega_i + \omega$, where ω is the frequency of the induced longitudinal oscillation. To obtain the growth rate due to the stimulated Raman scattering, we need to retain only the Stokes mode. (We discuss the effect of anti-Stokes mode later.) If we Fourier-transform eqs. (40) to (44), retaining only the Stokes mode, we have

$$\left\{k_s^2 - \frac{1}{c^2}[(\omega_i - \omega)^2 - \omega_p^2]\right\} \mathbf{E}_s = -i(\omega_i - \omega)\mu_0 e n_l^* \mathbf{v}_i, \tag{48}$$

where * shows the complex conjugate.

If we express n_1 in terms of $\mathbf{E}_1$, using Eqs. (46) and (47),

$$n_l = n_0 \frac{e}{m} \frac{\mathbf{k}_l \cdot \mathbf{E}_l}{i\omega^2}, \tag{49}$$

eq. (48) becomes

$$D_s(k_s, \omega_i - \omega)\mathbf{E}_s = \omega_s(\mathbf{k}_l \cdot \mathbf{E}_l^*)\mathbf{v}_i, \tag{50}$$

where

$$D_s(k,\omega) = k^2c^2 + \omega_p^2 - \omega^2, \tag{51}$$

and $\omega_l \simeq \omega_p$ is used in evaluating the right-hand side of (50). $D_s = 0$ gives the linear dispersion relation of the scattered electromagnetic wave. Equation (50) shows that the dispersion relation is modified by the incident electromagnetic wave and the induced longitudinal wave.

To close the equations, we now must express $\mathbf{E}_l$ in terms of $\mathbf{E}_s$ and $\mathbf{v}_i$. The set of equations that describe the longitudinal mode are Poisson's equation,

$$\nabla \cdot \mathbf{E}_l = -\frac{en_l}{\epsilon_0}, \tag{52}$$

and the continuity equation (46), both of which are linear, and the equation of motion,

$$\frac{d\mathbf{v}_l}{dt} = -\frac{e}{m}(\mathbf{E}_l + \mathbf{v}_i \times \mathbf{B}_s + \mathbf{v}_s \times \mathbf{B}_i). \tag{47'}$$

The continuity equation is linear because the electromagnetic wave is incompressible, $n_s = n_i = 0$. This means that the current density for the longitudinal mode is given by $-en_0\mathbf{v}_l$. Hence, the only nonlinearity comes from the Lorentz force, $\mathbf{v} \times \mathbf{B}$, in eq. (47′). Note that we dropped the corresponding nonlinear term in the calculation of $\mathbf{J}_s^{NL}$ because it is smaller than the term retained by the factor of v_i/c. Also note that we used the linear relation, eq. (47), to express n_l to evaluate the coupling term $n_l\mathbf{v}_i$ of (50) because it was a higher order correction there. If we use the Maxwell equation,

$$\omega\mathbf{B} = \mathbf{k} \times \mathbf{E}, \tag{53}$$

the nonlinear terms in (47′) become

$$\begin{aligned}
&(\mathbf{v}_i \times \mathbf{B}_s^* + \mathbf{v}_s^* \times \mathbf{B}_i) \\
&= \left(\mathbf{v}_i \times \frac{\mathbf{k}_s \times \mathbf{E}_s^*}{\omega_s} + \mathbf{v}_s^* \times \frac{\mathbf{k}_i \times \mathbf{E}_i}{\omega_i}\right) \\
&\simeq \frac{1}{\omega_s}(\mathbf{v}_i \cdot \mathbf{E}_s^*)(\mathbf{k}_s - \mathbf{k}_i) \\
&= -\frac{1}{\omega_s}(\mathbf{v}_i \cdot \mathbf{E}_s^*)\mathbf{k}_l,
\end{aligned} \tag{54}$$

where we used $\mathbf{k}_s \cdot \mathbf{v}_i = 0$. Hence the total longitudinal velocity modulation is given by

$$\mathbf{v}_l = \frac{1}{i\omega}\frac{e}{m}\left(\mathbf{E}_l - \frac{\mathbf{v}_i \cdot \mathbf{E}_s^*}{\omega_s}\mathbf{k}_l\right). \quad (55)$$

If we use this expression in (46) and (52), we have

$$D_l(k_l,\omega)\mathbf{k}_l \cdot \mathbf{E}_l = -k_l^2 \frac{\mathbf{v}_i \cdot E_s^*}{\omega_s}, \quad (56)$$

where

$$D_l(k,\omega) = 1 - \frac{\omega_p^2}{\omega^2}, \quad (57)$$

and $D_l = 0$ gives the linear dispersion relation for the longitudinal mode. Noting that $\mathbf{E}_s$ is parallel to $\mathbf{v}_i$ in eq. (50), eqs. (50) and (56) present the set of coupled equations between the scattered wave and the induced longitudinal wave,

$$D_s \mathbf{E}_s = \omega_s (\mathbf{k}_l \cdot \mathbf{E}_l^*)\mathbf{v}_i, \quad (50)$$

$$D_l \mathbf{k}_l \cdot \mathbf{E}_l = -k_l^2 \frac{\mathbf{v}_i \cdot \mathbf{E}_s^*}{\omega_s}\frac{\omega_p^2}{\omega^2}, \quad (56)$$

through the velocity modulation by the incident wave $\mathbf{v}_i$. The dispersion relation of the coupled system is given by eliminating $\mathbf{k} \cdot \mathbf{E}_l$ and $\mathbf{E}_s$ from these equations,

$$D_s(k_s,\omega_i - \omega)D_L(k_l,\omega) + \frac{\omega_p^2}{\omega^2} k_l^2 v_i^2 = 0. \quad (58)$$

If $k_l v_i$ is much smaller than ω_l, eq. (58) may be solved for a small frequency deviation $\Delta\omega$ from the frequency given by the linear dispersion relation by expanding D_s and D_L as

$$D_s(k_s,\omega_i - \omega) = D_s(k_s,\omega_s) + \left.\frac{\partial D_s}{\partial \omega}\right|_{k_s,\omega_s} \Delta\omega = 0 + 2\omega_s \Delta\omega, \quad (59)$$

while

$$D_l(k_l,\omega) = D_l(k_l,\omega_l) + \left.\frac{\partial D_l}{\partial \omega}\right|_{k_l,\omega_l} \Delta\omega = 2\Delta\omega/\omega_p. \quad (60)$$

Substituting (59) and (60) into (58), we have

$$\Delta\omega = \pm\frac{i}{2}|k_l v_i|\left(\frac{\omega_p}{\omega_s}\right)^{1/2}. \quad (61)$$

The imaginary part in $\Delta\omega$ gives the Raman growth rate in the beam frame Γ_B^R, hence

$$\Gamma_B^R = \frac{1}{2} |k_1 v_i| \cdot \left(\frac{\omega_p}{\omega_s}\right)^{1/2}. \tag{62}$$

In the case of the periodic magnetic pump, v_i is related to $B_\perp$ through eq. (45). The growth rate in this case is then given by

$$\Gamma_B^R = \frac{\gamma^2 e B_\perp}{\gamma_0 m} \left(\frac{\omega_p}{\omega_s}\right)^{1/2}. \tag{63}$$

The gain in the laboratory frame is simply given by $\Gamma_B/2\gamma$ as shown in eq. (29).

We note here that the ratio γ^2/γ_0 can be expressed in term of γ through (21),

$$\frac{\gamma^2}{\gamma_0} = \frac{\gamma_0}{1 + \gamma_0^2 v_{L\perp}^2/c^2}. \tag{64}$$

This expression indicates that a level exists in the velocity modulation $v_{L\perp}$, or the pump strength $B_\perp$, that produces a maximum growth rate. This is because an excessively large modulation deflects the beam too much in the transverse direction, which results in reducing the value of γ. There are different ways by which the growth rate can be optimized depending on the choice of fixed quantities. In any case, the maximum growth is achieved by selecting

$$v_{L\perp}^2 \, \gamma_0^2/c^2 \sim 1,$$

or in terms of the modulation magnetic field,

$$\frac{eB_\perp}{m} \frac{1}{k_0 c} = \frac{eB_\perp}{m} \frac{1}{\omega_0} \sim 1. \tag{65}$$

When the pump intensity is large such that the growth rate Γ_B becomes larger than the plasma frequency, that is, if

$$|k_1 v_i| > (\omega_p \omega_s)^{1/2}, \tag{66}$$

the longitudinal mode loses its linear property. In this regime, the growth rate should be obtained from (58) without expanding $D_l(k_1,\omega)$ around k_1,ω_p.[8] The growth rate is then modified to

$$\Gamma_B^0 = \left[\frac{\omega_p^2 k_1^2 v_i^2}{2\omega_i}\right]^{1/3}. \tag{67}$$

This regime is often called the oscillating two-stream instability (OTSI).[9]

If the pump amplitude is further increased, we should include the effect of the anti-Stokes mode which is simultaneously coupled in. The dispersion relation including the anti-Stokes mode becomes

$$1 + \frac{k_1^2 v_i^2 \omega_p^2}{D_l(k_1,\omega)\omega^2} \left[\frac{1}{D_s(k_s,\omega_i - \omega)} + \frac{1}{D_s(k_s^+,\omega_i + \omega)}\right] = 0, \tag{68}$$

where k_s^+ is the wave number of the scattered anti-Stokes mode. The growth rate in this regime is shown to be proportional to v_i^2, and it corresponds to the modulation instability (for example, see Ref. 10) of the pump wave.

V. STIMULATED COMPTON SCATTERING

Here we obtain the gain in the stimulated Compton regime. As was discussed in Section III, if the wave number of the longitudinal oscillation induced in the beam electrons is larger than the Debye wave number, $k_D(=\omega_p/v_T)$, the collective nature of the longitudinal mode is lost. The scattering then occurs by the individual electrons.

Because distribution of velocities exists in the beam electrons, to obtain the total scattering gain we must average over the velocity distribution. If we look at Fig. 3, we see that the resonant condition of the stimulated Compton scattering in the beam frame is given by

$$\omega_i - \omega_s = |k_l| v_T, \tag{69}$$

$$|k_i| + |k_s| = |k_l|. \tag{70}$$

As we have seen in the case of the stimulated Raman scattering, we must obtain J_s^{NL} to calculate the effect of the pump on the scattered mode in (40). In the present case, the Fourier amplitude of J_s^{NL} is again given by

$$J_s^{NL} = -en_l^* v_i; \tag{71}$$

however, the calculation of n_l^* is more complicated because of the averaging over the velocity distribution.

To obtain n_l^*, we use the Vlasov equation, which includes the nonlinear force term produced by the $\mathbf{v} \times \mathbf{B}$ force as seen previously.

$$\frac{\partial f_l}{\partial t} + v_z \frac{\partial f_l}{\partial z} + \frac{F_l^{NL}}{m} \frac{\partial f_0}{\partial v_z} = 0, \tag{72}$$

where f_l and f_0 are the perturbed (which represents the induced density modulation) and unperturbed velocity distribution function of electrons in the beam frame, v_z is the z component of velocity, and F_l^{NL} is the nonlinear force acting upon electrons at the frequency $\omega = \omega_l$,

$$F_l^{NL} = -e(\mathbf{v}_i \times \mathbf{B}_s + \mathbf{v}_s \times \mathbf{B}_i). \tag{73}$$

In (72), the linear force produced by the self-field, eE_l/m, is ignored because the induced longitudinal field is nonresonant; that is, $D_l(k_l,\omega_l) \neq 0$, due to the heavy Landau damping, and hence its amplitude is small. If we Fourier-transform eqs. (72) and (73) and take only the Stokes term, we have

$$f_l = \frac{\partial f_0/\partial v_z}{i(k_l v_z - \omega)} \frac{e}{m} \frac{k_l}{\omega_s} \mathbf{v}_i \cdot E_s^*. \tag{74}$$

The induced charge density n_l is then obtained by integrating this expression over v_z,

$$en_1 = i\frac{k_1^2\,\epsilon_0 \mathbf{v}_i \cdot \mathbf{E}_s^*}{\omega_s}\chi_1, \tag{75}$$

where χ_1 is the susceptibility of an electron gas,

$$\chi_1 = -\frac{\omega_p^2}{k_1^2}\int \frac{\partial f_0/\partial v_z}{v - (\omega + i0)/k_1} dv_z. \tag{76}$$

The dispersion relation for the scattered wave is now obtained by substituting (75) for the expression for the nonlinear current density, (71), and using it in the wave equation for the scattered electric field, (48).

$$[(\omega_i - \omega)^2 - \omega_p^2 - c^2 k_s^2]E_s$$
$$= |v_i|^2 \chi_1^* k_1^2 E_s. \tag{77}$$

If we solve for $\omega \simeq \omega_i - \omega_s + \Delta\omega$, we have

$$\Delta\omega = -\frac{\chi_1^*}{2\omega_s} k_1^2 |v_i|^2. \tag{78}$$

The temporal growth rate is obtained from the imaginary part of χ_1^*. From Eq. (76), we see

$$\text{Im}\,\chi_1 = -\frac{\chi_p^2}{k_1^2}\pi \int \delta(v - \omega/|k_1|)\frac{\partial f_0}{\partial v_z} dv_z. \tag{79}$$

If we take the Maxwellian velocity distribution for f_0 in the beam frame,

$$f_0 = \frac{1}{\sqrt{2\pi}\, v_T} e^{-v^2/2v_T^2}, \tag{80}$$

$$\text{Im}\,\chi_1 = \frac{\omega_p^2}{k_1^2 v_T^2}\sqrt{\frac{\pi}{2e}} \simeq 0.76\frac{\omega_p^2}{k_1^2 v_T^2}. \tag{79$'$}$$

The Compton growth rate Γ_B^c is now obtained from (78) and (79′),

$$\Gamma_B^c \simeq 0.4\frac{\omega_p^2}{\omega_s}\frac{|v_i|^2}{v_T^2}. \tag{81}$$

If we compare the Compton growth rate Γ_B^c with the Raman growth rate, (62), we see a qualitative difference. The Compton growth rate is proportional to the pump amplitude squared, while the Raman growth rate is proportional to the pump amplitude itself.

If the pump amplitude is increased such that $v_i > v_T$, it has been shown by Hasegawa et al.[11] that the pump field effectively increases the velocity spread by $\mathbf{v}_i \times \mathbf{B}_i$ force and thus decreased the gain. The proof was made for an electromagnetic wave pump, but it is believed that even when the helical magnetic pump is used, the similar effect appears when the beam enters into the magnetic field and suddenly see the magnetic field pressure, $B_1^2/2\mu_0$. The Compton gain for such a case becomes[11]

$$\Gamma_B^c \simeq 0.3\frac{\omega_p^2}{\omega_s}\frac{v_i}{c}\left(\frac{c}{v_T}\right)^{3/2}. \tag{82}$$

One important remark should be made here. We obtained Raman and Compton gains by taking the asymptotic limits of $k_l \ll k_D$ and $k_l \gg k_D$, respectively, to have simple analytic expressions. However, this does not mean that the gain at the transition regime cannot be obtained, nor that an abrupt transition exists between the two regimes. In fact, the unified dispersion relation which covers the entire regime can be obtained by using the Vlasov equation and by simply including the self-consistent electric field $\mathbf{E}_l$ in (72). If we further allow a situation that the scattered wave may not propagate in the beam direction, the unified dispersion relation which is expressed in the form of eq. (68) becomes

$$1 - \frac{k_l^2 \chi_l^* (k_l,\omega)}{1 + \chi_l^* (k_l,\omega)} \left[\frac{|\mathbf{k}_s \times \mathbf{v}_i|^2}{k_s^2 D_s(k_s,\omega_i - \omega)} + \frac{|\mathbf{k}_s^+ \times \mathbf{v}_i|^2}{k_s^{+2} D_s(k_s^+,\omega_i + \omega)} \right] = 0. \quad (83)$$

The gain for the entire regime is obtained by numerically solving this equation for ω.

VI. LIMITING GAIN AND OUTPUT POWER

In the previous two sections, temporal growth rates for stimulated Raman and stimulated Raman scatterings were obtained. We summarize the result in the following, by using $k_l \simeq 2|k_i| \simeq 2\omega_s/c$, and $\omega_s \sim \omega_i$.

Raman gain (beam frame)

$$\Gamma_B^R = \frac{|v_i|}{c} (\omega_p \omega_i)^{1/2}, \qquad \text{if } \frac{|v_i|}{c} \ll \left(\frac{\omega_p}{\omega_i}\right)^{1/2}, \quad (84)$$

$$\Gamma_B^0 = \left(2 \frac{|v_i|^2}{c^2} \omega_p^2 \omega_i\right)^{1/3}, \qquad \text{if } \frac{|v_i|}{c} \gg \left(\frac{\omega_p}{\omega_i}\right)^{1/2}. \quad (85)$$

Compton gain (beam frame)

$$\Gamma_B^c = 0.4 \frac{|v_i|^2}{v_T^2} \frac{\omega_p^2}{\omega_i}, \qquad \text{if } \frac{v_i}{v_T} < 1, \quad (86)$$

$$\Gamma_B^c = 0.3 \frac{|v_i|}{c} \frac{\omega_p^2}{\omega_i} \left(\frac{c}{v_T}\right)^{3/2}, \qquad \text{if } \frac{v_i}{v_T} > 1. \quad (87)$$

The gain in all cases depends on the pump intensity v_i. If one uses the helical magnetic pump, as we have shown in Section VI, an optimum value exists in the pump magnetic field $B_\perp$, which is given by eq. (64). The corresponding velocity v_i becomes $|v_i|/c \simeq 1/\sqrt{2}$. If we use this value, the Raman (OTSI) and Compton gains become

$$\Gamma_{B\max}^R \simeq (\omega_p^2 \omega_i)^{1/3}, \quad \text{applicable for } \omega_i \ll \frac{\gamma}{2\Delta\gamma} \omega_p, \quad (88)$$

$$\Gamma_{B\max}^c \simeq 0.2 \left(\frac{\gamma}{\Delta\gamma}\right)^{3/2} \frac{\omega_p^2}{\omega_i}, \quad \text{applicable for } \omega_i \gg \frac{\gamma}{2\Delta\gamma} \omega_p. \quad (89)$$

Here $\omega_i = 2\Delta\gamma/\gamma\, \omega_p$ corresponds to the critical frequency, eq. (37) between the two regimes, that is the incident frequency for $k_l = k_D$.

We see that the growth rate increases gradually as ω_i is increased and then decreases in proportion to ω_i^{-1}. If we take an example of a best quality beam with $\Delta\gamma \sim 10^{-3}\,\gamma$, $\Gamma^c_{B\,\max}$ at the critical frequency is given approximately by

$$\Gamma^c_{B\,\max} \simeq 0.4\,\omega_p \left(\frac{\gamma}{\Delta\gamma}\right)^{1/2} \simeq 12\,\omega_p.$$

On the other hand, at the same frequency,

$$\Gamma^R_{B\,\max} \sim \omega_p \left(\frac{\gamma}{2\Delta\gamma}\right)^{1/3} \simeq 7.8\,\omega_p.$$

This indicates that, at the critical frequency, the Raman and Compton gains are approximately the same. If we now express the plasma frequency in terms of the beam current density J_0, $\omega_p = 8.14 \times 10^6 \sqrt{J}$, hence the maximum growth rate in the beam frame is approximately given by $\Gamma_{B\,\max} \sim 10\,\omega_p \sim 10^8 \sqrt{J}$. As an example, if we take a nominal parameter of "microtron" [12] beam with a current of 1 A with the cross section of 1 mm^2, $J = 10^6$ A/m^2. Thus, $\Gamma_{B\,\max} \simeq 10^{11}$ sec^{-1}. We also note that the gain in the laboratory frame Γ_L is given by $\Gamma_B/2\gamma$. For a nominal value of $\gamma = 10^3$, the laboratory frame gain is 5×10^8 sec^{-1}. Hence the e-folding distance $L = c/\Gamma_L \simeq 1$ m. The e-folding distance at a lower frequency becomes shorter in proportion to $\omega_i^{-1/3}$, while at a higher frequency becomes longer in proportion to ω_i.

These arguments may be summarized as follows. If we define the critical frequency given by (37) as the limiting frequency that the free electron laser can operate, the minimum e-folding distance in the laboratory frame L_m and ω_{cr} can be expressed in terms of J_0, γ and $\gamma/\Delta\gamma$.

The maximum lasing frequency, f_{cr}:

$$f_{cr} = \frac{\omega_{cr}}{2\pi} = 1.3 \times 10^6\,\gamma \left(\frac{\gamma}{\Delta\gamma}\right) [J_0(\mathrm{A/m^2})]^{1/2}\ \mathrm{Hz}. \tag{90}$$

The minimum e-folding distance, L_m:

$$L_m = \frac{c}{\Gamma_{L\,\max}} = 93\gamma \left(\frac{\Delta\gamma}{\gamma}\right)^{1/3} [J_0(\mathrm{A/m^2})]^{1/2}\ \mathrm{m}. \tag{91}$$

Condition to achieve L_m:

$$\frac{eB_\perp}{m} = k_0 c = \frac{\omega_{cr}}{2\gamma^2}$$

or

$$B_\perp(W/m^2) = 1.8 \times 10^{-11} \frac{f_{cr}}{\gamma^2}. \tag{92}$$

Note that the beam pulse length (Fig. 1) is not a crucial parameter so long as it is longer than, say, $10\,k_1^{-1}$ because it runs at the same speed as the scattered light. If we take again the previous examples of microtron,[12] $J_0 = 10^6\ \mathrm{A/m^2}$, $\gamma = 10^2$, and $\gamma/\Delta\gamma = 10^3$, we have

$$f_{cr} = 1.3 \times 10^{14}\ \mathrm{Hz}$$

$$L_m = 0.93\ \mathrm{m}$$

$$B_\perp = 2.3 \times 10^{-1}\ \mathrm{W/m^2}$$

$$\lambda_0 = 2\pi/k_0 = \frac{2\gamma^2 c}{f_{cr}} = 4.6 \times 10^{-2}\ \mathrm{m}.$$

Let us now discuss the maximum output power of the laser. Because L_m is on the order of 1 m, it takes a relatively long system to achieve the saturation in gain. But let us assume that the system is infinitely long and ask ourselves what causes the saturation of the gain.

As we have found, when the energy spread of the beam becomes large so that $k_1 < k_D$, the gain drops in proportion to ω_i^{-1}. When the scattered power is increased, it produces a larger $\mathbf{v} \times \mathbf{B}(= \mathbf{v}_i \times \mathbf{B}_s)$ force which traps the beam electrons and increases its energy spread. The trapping potential ϕ_t due to the Lorentz force $\mathbf{v}_i \times \mathbf{B}_s$ in the beam frame is obtained from

$$\left|\frac{\partial \phi_t}{\partial z}\right| = |k_1 \phi| \simeq |v_i B_s^*|$$

or

$$\phi_t = \frac{1}{k_1} |v_i| |B_s|. \tag{93}$$

The effective thermal speed v_{Teff} produced by the trapping potential ϕ_t is

$$v_{\mathrm{Teff}} = \left(\frac{2e\phi_t}{m}\right)^{1/2}. \tag{94}$$

We can consider that the saturation occurs when $k_1 \simeq \omega_p/v_{\mathrm{Teff}}$ because if v_{Teff} is made larger than this critical value, the gain changes from Raman to Compton. Hence, the maximum amplitude of the magnetic field of the scattered wave is given by

$$k_1 = \frac{\omega_p}{(2e\phi_t/m)^{1/2}} = \frac{\omega_p}{(2e|v_i||B_s|/k_1 m)^{1/2}}, \tag{95}$$

or by solving B_s using $|v_i| \simeq c$, we have

$$B_s = \frac{m}{e}\frac{\omega_p^2}{ck_i} = \frac{m}{e}\frac{\omega_p^2}{\omega_i}. \tag{96}$$

If we operate at the maximum gain, $\omega_i = \omega_{cr}/2\gamma = \omega_p(\gamma/\Delta\gamma)/2$. Hence, we must use as the maximum scattered field

$$B_s = 2\frac{m}{e}\omega_p\frac{\Delta\gamma}{\gamma}, \tag{97}$$

and the corresponding electric field is

$$E_s = cB_s. \tag{98}$$

If we Lorentz-transform these fields to the laboratory frame according to eqs. (5) and (7), we have

$$B_{Ls} = 2\gamma B_s$$

and

$$E_{Ls} = 2\gamma E_s. \tag{99}$$

Hence, the maximum output power P_m is given by

$$\begin{aligned} P_m &= E_{Ls}B_{Ls}/\mu_0 \\ &= 16\gamma^2 \left(\frac{m}{e}\right)^2 \omega_p^2 \left(\frac{\Delta\gamma}{\gamma}\right)^2 \frac{c}{\mu_0} \\ &= 16 \left(\frac{\Delta\gamma}{\gamma}\right)^2 P_{\text{Beam}}, \end{aligned} \tag{100}$$

where P_{Beam} is the beam kinetic power density,

$$P_{\text{Beam}} = mc^3\gamma n. \tag{101}$$

Equation (100) shows that the conversion efficiency is roughly given by $16(\Delta\gamma/\gamma)^2$. This may be misleading, because it shows that the poorer quality beam gives better efficiency. This comes from the dependency of B_s on ω_i^{-1} so that the lower the frequency the longer the saturation field. When a poor quality beam is used, the efficiency may become better but with a sacrifice of lowering the laser frequency.

If we use the same example of parameters, $\gamma = 10^2$, $\Delta\gamma/\gamma = 10^{-3}$ and 1 A beam, the maximum output power of the laser becomes 800 W.

VII. CONCLUSION

Use of stimulated backscattering of a pump field by a relativistic electron beam for a tunable laser was discussed. The temporal gain and the e-folding distance in the laboratory frame are obtained for both stimulated Raman and stimulated Compton scattering regimes. It is shown that in the stimulated Compton regime, the gain drops in proportion to the lasing frequency hence is not a practical regime to deploy. If we consider that the transition frequency from the Raman to the Compton regime is the maximum lasing frequency, the lasing frequency can be obtained as a function of the beam energy γ, the relative energy spread of the beam $\Delta\gamma/\gamma$, and the current density J_0 as shown in (90). The e-folding distance corresponding to this frequency is shown in eq. (91). For a nominal value of the available relativistic electron beam, these quantities become approximately 10^{14} Hz and 1 m. The maximum power output corresponding to this operation condition is also obtained and shown to be given by (100). Again for the nominal value of the beam parameter, the output laser power becomes about one kilowatt. These results indicate that the use of a relativistic beam with γ of 100 and $\Delta\gamma/\gamma$ of 10^{-3} can produce a tunable laser with an optimum operating frequency approaching to the visible. However, extending this process into X-ray regime seems extremely difficult.

VIII. ACKNOWLEDGMENTS

The author would like to thank B. M. Kincaid for his interest in this problem and many valuable discussions on available experimental data, and to H. Ikezi and K. Mima for valuable technical discussions.

REFERENCES

1. V. L. Granatstein, S. P. Schlesinger, M. Herndon, R. K. Parker, and J. A. Pasour, "Production of Megawatt submillimeter pulses by Stimulated Magneto-Raman Scattering," App. Phys. Lett., *30* (1977), pp. 384–386.
2. D. A. G. Deacon, L. R. Elias, J. M. J. Madey, G. R. Ramian, H. A. Schwettman, and T. I. Smith, "First Operation of Free Electron Laser," Phys. Rev. Lett., *38*, pp. 892–894.
3. L. D. Landau and E. M. Lifshitz, *The Classical Theory of Field,* New York: Pergamon Press, 1975, pp. 9–65.
4. V. N. Tsytovich, "*Nonlinear Effects in Plasma*," New York: Plenum Press, 1970.
5. P. K. Kaw, W. L. Kruer, C. S. Lin, and K. Nishikawa, "Parametric Instabilities in Plasma," *Advances in Plasma Physics,* Vol. 6, Ed. by A. Simon and W. B. Thompson, New York: Academic Press, 1976, pp. 1–270.
6. P. Sprangle and A. T. Drobot, "Stimulated Backscattering from Relativistic Unmagnetized Electron Beams," Proc. Free Electron Generators of Coherent Radiation Workshop, Telluride, Colorado, August 17–21, 1977.
7. F. A. Hopf, P. Meystre, M. O. Scully, and W. H. Louisell, "Strong-Signal Theory of a Free Electron Laser," Phys. Rev. Lett., *37* (1977) pp. 1342–1944.
8. V. P. Silin, "Parametric Resonance in a Plasma," Sov. Phys. JETP, *21* (1965) pp. 1127–1134, and K. Nishikawa, "Parametric Excitation of Coupled Waves, I, General Formulation," J. Phys. Soc. Japan, *24* (1968) pp. 916–922.
9. J. Drake, P. Kaw, Y. C. Lee, G. Schmidt, C. S. Liu, and M. N. Rosenbluth, "Parametric Instabilities of Electromagnetic Waves in Plasmas," Phys. Fluids, *17* (1974), pp. 778–785.
10. A. Hasegawa, *Plasma Instabilities and Nonlinear Effects,* Heidelberg: Springer-Verlag 1975, pp. 201–204.
11. A. Hasegawa, K. Mima, P. Sprangle, H. H. Szu, and V. L. Granatstein, "Limitation in Growth Time of Stimulated Compton Scattering in X-ray Regime," Appl. Phys. Lett., *29,* (1976), pp. 542–544.
12. P. M. Lapstolle and A. L. Septier, eds. *Linear Accelerators,* North-Holland, 1970, pp. 553–567.